[4]Ericsson, L. E., "Difficulties in Predicting Vortex Breakdown Effects on a Rolling Delta Wing," *Journal of Aircraft*, Vol. 33, No. 3, 1996, pp. 477–484.
[5]Atta, R., and Rockwell, D., "Hysteresis of Vortex Development and Breakdown on an Oscillating Delta Wing," *AIAA Journal*, Vol. 25, No. 11, 1987, pp. 1512, 1513.
[6]Ericsson, L. E., and Reding, J. P., "Fluid Dynamics of Unsteady Separated Flow, Part II, Lifting Surfaces," *Progress in Aerospace Sciences*, Vol. 24, 1987, pp. 249–356.
[7]Beyers, M. E., private communication, July 1994.
[8]Ericsson, L. E., and King, H. H. C., "Effect of Cross-Sectional Geometry on Slender Wing Unsteady Aerodynamics," *Journal of Aircraft*, Vol. 30, No. 5, 1993, pp. 793–795.
[9]Lambourne, N. C., Bryer, D. W., and Maybrey, J. F. M., "The Behavior of the Leading Edge Vortices over a Delta Wing Following a Sudden Change of Incidence," Aeronautical Research Council, R&M 3645, England, UK, March 1969.
[10]Elle, B. J., "An Investigation at Low Speed of the Flow near the Apex of Thin Delta Wings with Sharp Leading Edges," Aeronautical Research Council, R&M 3176, England, UK, Jan. 1958.
[11]Ericsson, L. E., and Reding, J. P., "Approximate Nonlinear Slender Wing Aerodynamics," *Journal of Aircraft*, Vol. 14, No. 12, 1977, pp. 1197–1204.
[12]Lambourne, N. C., and Bryer, D. W., "The Bursting of Leading-Edge Vortices—Some Observations and Discussion of the Phenomenon," Aeronautical Research Council, R&M 3282, England, UK, April 1961.

Numerical Approach to Blade–Vortex Interaction in Two-Dimensional Viscous Flow

Bonian Dong*
Singapore Technologies Aerospace, 539938 Singapore
and
Y. T. Chew† and B. C. Khoo‡
National University of Singapore, 119260 Singapore

Introduction

In the previous two-dimensional viscous study on the blade–vortex interaction, the total flowfield is obtained through the interaction between the vortex-induced flow and the viscous flow around the stationary airfoil.[1,2] The shortcoming of such an interaction scheme is that the viscous effect of the passing vortex is not taken into consideration in the viscous solution. The purpose of this work is to introduce a numerical approach that includes the passing vortex in the viscous solution. The calculation is started in a manner similar to the one used by Wu et al.[1] and Hsu and Wu,[2] except that, in this work, the passing vortex is modeled as a cluster of point vortices. Based on the concept of the vortex-in-cell (VIC) method for inviscid flows,[3] a specially devised vorticity distribution scheme is used when the passing vortex is close to the stationary airfoil. In this scheme, the cluster of point vortices becomes a continuous vortical patch after being linearly distributed in a weighted manner. Then the total flow is solved by the Navier–Stokes equations, and the viscous effect of the passing vortex on the blade–vortex interaction can be investigated.

Received June 26, 1994; revision received Nov. 1, 1995; accepted for publication Dec. 10, 1995.

*Research Engineer, Engineering Development Center.
†Associate Professor, Department of Mechanical and Production Engineering.
‡Senior Lecturer, Department of Mechanical and Production Engineering.

Equations and Numerical Schemes

The problem is stated as follows: the steady flowfield around a stationary airfoil is disturbed by a passing vortex released from upstream, and then the resulting unsteady flowfield is studied.[2]

The unsteady incompressible Navier–Stokes equations in the form of a vorticity-stream function for two-dimensional flows are

$$\frac{\partial^2\psi}{\partial x^2} + \frac{\partial^2\psi}{\partial y^2} = -\omega$$
$$\frac{\partial\omega}{\partial t} + \frac{\partial\psi}{\partial y}\frac{\partial\omega}{\partial x} - \frac{\partial\psi}{\partial x}\frac{\partial\omega}{\partial y} = \frac{1}{Re}\left(\frac{\partial^2\omega}{\partial x^2} + \frac{\partial^2\omega}{\partial y^2}\right) \tag{1}$$

where ψ is the stream function, ω is the vorticity, and Re is the Reynolds number based on the airfoil chord length and freestream velocity. On the solid wall, the boundary conditions are

$$\psi_w = 0$$
$$\omega_w = -\left.\frac{\partial^2\psi}{\partial n^2}\right|_w \approx -\frac{2(\psi_1 - \psi_w)}{h^2} \tag{2}$$

where n is the local normal coordinate, and the subscripts w and 1 indicate the wall and the first point at the distance of h from the wall, respectively. The first-order discretization for ω in Eq. (2) is used in the numerical solution to keep the total vorticity of the flow conserved as discussed by Wu.[4] On the far-field boundary, ω and ψ take the values of the freestream. The linear triangular finite element method[5] on a C-grid is used to calculate the viscous flow surrounding the stationary airfoil, and no artificial viscosity is applied.

Interaction Scheme

This scheme is similar to the one used by Wu et al.[1] and Hsu and Wu,[2] who used only one point vortex to represent the passing vortex, but in this work, a cluster of point vortices is used.[6] The stream function of total flow can be decomposed as two parts: 1) the vortex-induced flow ψ_Γ and 2) the disturbed viscous flow ψ_V. Here, ψ_Γ is evaluated by the Biot–Savart law[1] and ψ_V is solved by substituting $\psi = \psi_V + \psi_\Gamma$ into Eq. (1) and utilizing the boundary conditions. The passing vortex is made to convect at the local fluid speed. In this scheme, the passing vortex is not included in the viscous solution.

Distribution Scheme

In the linear triangular finite element calculation, ω_0 at a node represents a linear vorticity distribution on the six elements that share the same node as shown in Fig. 1a, and the circulation (positive clockwise) around these six elements is

$$\Gamma_0(\omega_0) = -\frac{\omega_0}{3}\sum_{k=1}^{6} A_k \tag{3}$$

where A_k is the area pertaining to element k as shown in Fig. 1a. For a point vortex located in an element, its vorticity strength is approximated by ω_1, ω_2, and ω_3 at the three nodes of the element. In this way, the point vortex becomes a vortical patch occupying the element where it is located and also the 12 adjacent elements as shown in Fig. 1b. The values of ω_1, ω_2, and ω_3 are weighted as follows:

$$\omega_1/a_1 = \omega_2/a_2 = \omega_3/a_3 \tag{4}$$

where a_1, a_2, and a_3 are subareas of the element as shown in

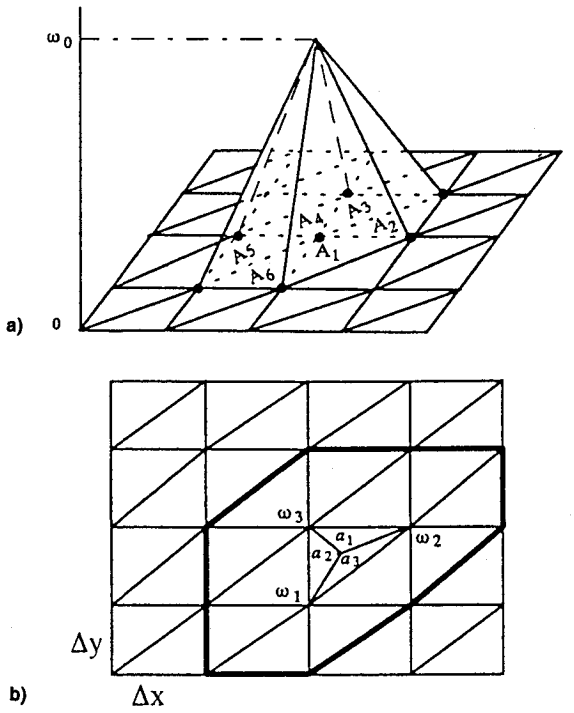

Fig. 1 a) Nonzero ω_0 at a node represents a linear vorticity distribution over the six elements and b) a point vortex in an element is distributed over the elements enclosed by the bold line.

Fig. 1b. To keep the circulation of the point vortex Γ unchanged, the following condition is imposed:

$$\Gamma = \Gamma_1(\omega_1) + \Gamma_2(\omega_2) + \Gamma_3(\omega_3) \tag{5}$$

where Γ_1, Γ_2, and Γ_3 are evaluated according to Eq. (3). The resulting vortical patch is superposed upon the vorticity field obtained from the viscous calculation so that the total flow including the passing vortex can be solved by the Navier–Stokes equations.

Numerical Example and Discussion

The parameters of the numerical example are taken from the wind-tunnel test of Straus et al.[7] and nondimensionalized by the freestream velocity and chord length of the stationary airfoil. The passing vortex, which is the wake generated by the sudden pitch of a NACA 0018 airfoil of length 0.54, passes the upper surface of a stationary NACA 0012 airfoil of unit length at zero angle of attack; it has a strength (circulation) of -0.15 (positive clockwise) and an initial vertical spacing of 0.24 above the stationary airfoil. In the numerical example, the passing vortex, which is a cluster of point vortices obtained by using the vortex panel method,[6] is introduced at an upstream location, 0.24 above and 5.0 away from the leading edge of the stationary airfoil without the presence of the pitching airfoil. The flow is laminar and $Re = 5 \times 10^3$.

The calculation starts with the interaction scheme. When the passing vortex is close to the leading edge of the airfoil, the distribution scheme takes over, whereby the passing vortex forms a continuous vortical patch as shown in Fig. 2a. The vorticity intensity of the passing vortex becomes weaker as it convects downstream (see Fig. 2b). This indicates that the passing vortex as a continuous vortical patch spreads out, and that its vorticity strength diffuses over a larger region.

In Fig. 3, the history of the numerically calculated lift coefficient C_L and moment coefficient C_M (positive clockwise about the leading edge) is compared to the experimental results of Straus et al.[7] The contribution of the shear stress to the lift and moment is excluded since only the pressure was measured in the experiment. As shown in Fig. 3, the lift and moment predicted by the interaction scheme agree well with the experimental data before the passing vortex gets close to the airfoil, but, when it is very close to the airfoil, the loading is overpredicted. On the other hand, the results of the distribution scheme agree well when the passing vortex is very close to the airfoil. As also shown in Fig. 3, the results of the interaction scheme and the distribution scheme agree closely with each other for a short period of time immediately after the introduction of the distribution scheme, and the results diverge only when the passing vortex gets even closer to the airfoil. This observation implies that the viscous diffusion of the passing vortex only manifests its importance on the blade–vortex interaction in the strong viscous region near the solid surface, and that it is not necessary to use the distribution scheme when the passing vortex is in a relatively less viscous region.

The accuracy and smoothness of the transition from the interaction scheme to the distribution scheme depend on the grid

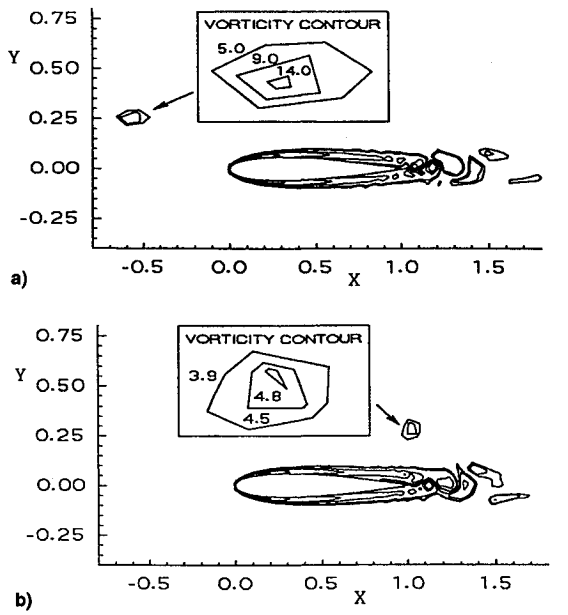

Fig. 2 Vorticity contour. The passing vortex is a) approaching the leading edge of the airfoil and b) passing the trailing edge of the airfoil.

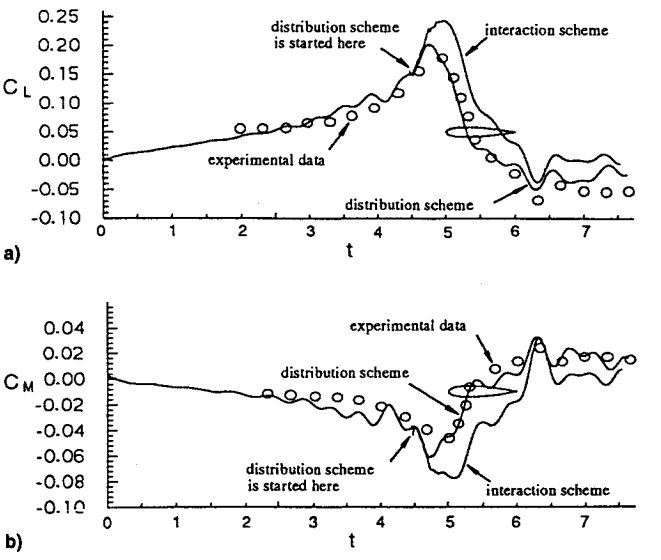

Fig. 3 Comparison between the numerical results and the experimental results.[7] The history of the a) lift coefficient and b) moment coefficient.

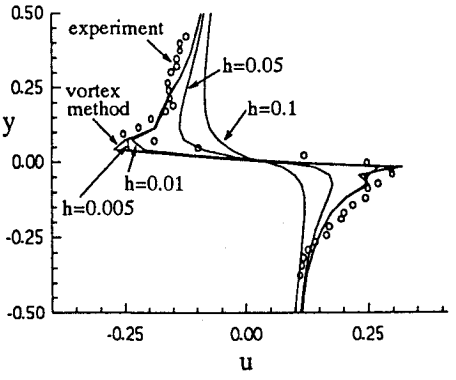

Fig. 4 For grids of different size, the computed streamwise velocity profiles across a relatively isolated vortex core are compared with the experimental result.[7]

size. When only one point vortex is distributed over the elements by the distribution scheme as shown in Fig. 1b, the numerical diffusion (error) will be introduced. But for a cluster of point vortices occupying a finite area, this error can be minimized if the grid size is small enough so that the resulting vortical patches, overlapping each other, occupy about the same region as the cluster does. In Fig. 4, the velocity profiles across a relatively isolated vortex core generated by a pitching airfoil are compared. A cluster of point vortices is generated by using the vortex panel method,[6] and, across it, the calculated velocity profile agrees well with the experimental result of Straus et al.[7] By the distribution scheme, the point vortices in the cluster are then distributed on the uniform grids of different size ($\Delta x = \Delta y = h$ and $h = 0.1$, 0.05, 0.01, and 0.005). For a finer grid size ($h \leq 0.01$), the velocity profiles obtained by the distribution scheme agree well with the experimental result[7] as shown in Fig. 4. In the numerical example presented in this section, the passing vortex is turned into a vortical patch by the distribution scheme in the vicinity of the stationary airfoil, where the grid size is less than 0.01, to ensure the accurate and smooth transition.

Summary

In this work, the distribution scheme is used to model the passing vortex as a continuous, viscous vortical patch, and the total flow including the passing vortex is governed by the Navier–Stokes equations. When the distribution scheme is applied to a cluster of point vortices on a fine-enough grid, the introduced numerical error can be minimized. The numerical results show that the effect of viscous diffusion of the passing vortex only manifests its importance on the blade–vortex interaction near the stationary airfoil.

References

[1]Wu, J. C., Hsu, T. M., Tang, W., and Sankar, L. N., "Viscous Flow Results for the Vortex-Airfoil Interaction Problem," AIAA Paper 85-4053, Oct. 1985.

[2]Hsu, T.-M., and Wu, J. C., "Theoretical and Numerical Studies of a Vortex-Airfoil Interaction Problem," AIAA Paper 86-1094, May 1986.

[3]Sarpkaya, T., "Computational Methods with Vortices—The 1988 Freeman Scholar Lecture," *Journal of Fluids Engineering*, Vol. 111, March 1989, pp. 5–51.

[4]Wu, J. C., "Numerical Boundary Conditions for Viscous Flow Problems," *AIAA Journal*, Vol. 14, No. 8, 1976, pp. 1042–1049.

[5]Baker, A. J., "Finite Element Computational Fluid Mechanics," Hemisphere, New York, 1983, pp. 101–103.

[6]Mook, D. T., and Dong, B., "Perspective: Numerical Simulations of Wakes and Blade-Vortex Interaction," *Journal of Fluids Engineering*, Vol. 116, No. 1, 1994, pp. 5–21.

[7]Straus, J., Renzoni, P., and Mayle, R. E., "Airfoil Measurements During a Blade Vortex Interaction and Comparison with Theory," *AIAA Journal*, Vol. 28, No. 2, 1990, pp. 222–228.

Mathematical Simulation of Near-Vertical Flight of Fixed-Wing Aircraft

Johan Ernest Mebius*
Delft University of Technology, 2600 Delft, The Netherlands

Nomenclature

$OXYZ$	=	Earth-fixed coordinate system
$oxyz$	=	body axes coordinate system
p, q, r	=	body axes components of angular velocity vector
p_n, p_z	=	tangent planes to S at N and Z, respectively
S, N, Z	=	fictitious sphere having its center at the aircraft's c.g., and its nadir and zenith poles
$SO(3)$	=	set of all three-dimensional attitudes; set of all three-dimensional rotations about a fixed point
δ	=	$\psi - \phi$
λ_n, μ_n, σ	=	nadir coordinates
λ_z, μ_z, δ	=	zenith coordinates
σ	=	$\psi + \phi$
ψ, θ, ϕ	=	Euler angles of rotation from Earth-fixed to body axes coordinate system

Introduction

IN the mathematics of flight simulation two methods are commonly used to represent the aircraft attitude, the one based on Euler angles, the other based on Euler parameters and the accompanying quaternion calculus.

Euler angles have an immediate intuitive appeal and are perfectly adequate for simulations in which one stays well clear of vertical attitudes. The singularities occurring in vertical aircraft attitudes constitute a major drawback of Euler angles, which makes them unsuitable for military flight simulation and for the analysis of flight incidents and accidents in which loss of control is a major factor.

Existing software for civil flight simulation employs Euler angles. An upgrade of this software to cover out-of-control situations and other situations with arbitrarily steep pitches may be done by replacing Euler angles with Euler parameters, but doing so requires a virtually system-wide reconstruction of the software.

This Note presents a mathematical method of eliminating in turn the singularity at vertical nose-down attitudes and the singularity at vertical nose-up attitudes (simply denoted as nose-down and nose-up, respectively). This method involves the introduction of a pair of new coordinate systems for aircraft attitudes, both of them based directly on Euler angles. The one system has a singularity only at nose-up attitudes; in this Note it is denoted as the nadir system; the other only at nose-down attitudes; this is called the zenith system. For the entire method the term extended Euler angles system is proposed.

One may employ a combination of the traditional Euler angles system and the nadir and zenith coordinate systems; with an appropriate switching scheme one avoids all singularities. Flight simulation software systems thus constructed would be more complex than systems based on Euler parameters, but it is expected that the introduction of the extended Euler angles system is far easier, both from a mathematical and a software engineering viewpoint, than a conversion to Euler parameters.

Received Jan. 21, 1995; revision received Dec. 15, 1995; accepted for publication Jan. 2, 1996.

*Assistant Professor, Department of Technical Mathematics and Informatics, P.O. Box 356. e-mail: j.e.mebius@twi.tudelft.nl.